MATERIALS RESEARCH SOCIETY
SYMPOSIUM PROCEEDINGS VOLUME 411

Electrically Based Microstructural Characterization

Symposium held November 27–30, 1995, Boston, Massachusetts, U.S.A.

EDITORS:

Rosario A. Gerhardt
Georgia Institute of Technology
Atlanta, Georgia, U.S.A.

S. Ray Taylor
University of Virginia
Charlottesville, Virginia, U.S.A.

Edward J. Garboczi
National Institute of Standards and Technology
Gaithersburg, Maryland, U.S.A.

PITTSBURGH, PENNSYLVANIA

ELECTRICAL CONDUCTION IN RELATION TO LOCAL AND INTERMEDIATE RANGE STRUCTURE OF RUBIDIUM GERMANATE GLASSES

H. Jain*, E.I. Kamitsos**, W. C. Huang* and Y.D. Yiannopoulos**
*Department of Materials Science and Engineering, Lehigh University, Bethlehem, PA 18017
**National Hellenic Research Foundation, Athens 11635, Greece.

ABSTRACT

The dependence of dc electrical conductivity of a series of rubidium germanate glasses on rubidium oxide concentration is correlated with the structural information obtained from extended x-ray absorption fine structure analysis, density, x-ray photoelectron, Raman and far infrared absorption spectroscopy. Previously macroscopic molar or excess volume showed the most obvious correlation with the activation energy of conductivity. The present results demonstrate additional importance of the intermediate range structure.

INTRODUCTION

The common oxide glasses such as alkali silicates, borates, germanates, phosphates conduct electricity via alkali ion transport. The ionic conductivity of such glasses is a very strong function of alkali ion concentration [1], indicating a strong influence of the structure on the conduction process. However, one does not readily observe any microstructural features in common homogeneous oxide glasses by optical or electron microscopy. Therefore, unlike for many crystalline materials, local and perhaps intermediate range structure should be crucial for ion transport in glass [2]. In general for simplicity we may consider the chemical and physical structure of the glass separately although the two are intimately related. The significance of the chemical structure for electrical properties of glasses has been discussed in another paper in this volume [3]. Therefore, in this paper we focus on the physical and vibrational structures which refer to the relative positions of the different atoms and the strength of the various bonds, respectively. By establishing a correlation between ionic conductivity and these structures, we hope to attain the objectives of these proceedings for glassy ionic conductors.

We have selected the rubidium germanate glass series for three reasons: (a) Recently, considerable structural information has been obtained for this system from x-ray photoelectron spectroscopy (XPS) [4,5], extended x-ray absorption fine structure (EXAFS) analysis [5], and far infrared (IR) and nuclear magnetic resonance (NMR) spectroscopy [6], making it one of the best characterized alkali oxide glass system. (b) This glass system shows 'germanate anomaly' such that its physical properties do not vary monotonously with increasing Rb_2O concentration [7]. Therefore, the results for this glass series provide a critical test of the models developed for normal alkali silicate glass systems. (c) The germanate glasses are potential materials for low-loss optical applications such as optical fibers and IR transmitting windows [8]. They are also potential candidates for Raman fiber-optical amplifiers [9,10].

EXPERIMENT

Sixteen $xRb_2O - (1-x)GeO_2$ glass compositions were selected with x = 0.00, 0.01, 0.02, 0.05, 0.10, 0.15, 0.20, 0.25, 0.30, 0.33, 0.37, 0.40, 0.45, 0.50, 0.55 and 0.60. The samples were prepared by the melt-quench method by mixing, preheating at 900 to 1000 °C for 1 hour and then melting in a platinum crucible appropriate amounts of GeO_2 (99.999%) and Rb_2CO_3 (99.8%) powders. The liquid

was equilibrated for about 1 hour at a temperature between 1200 and 1450 °C depending on composition and viscosity. Homogenized bubble free liquid was cast in a stainless steel mold and then the glass was annealed at ~ 450 °C for ~ 1/2 hour to remove internal stress before furnace cooling to room temperature. The resulting samples were cut into thin plates for XPS, IR and Raman spectroscopy and electrical conductivity measurements. They were ground into fine powders for EXAFS experiments.

The experimental procedures for the density, XPS, EXAFS, far IR and electrical conductivity measurements on the present samples have been described previously [5,6,11]. Raman spectra of the samples were recorded at room temperature on a Ramanor HG 2S Jobin-Yvon spectrometer using the 488.0 nm argon ion laser (500 mW Spectra Physics 165 model) line, with a 90^0 scattering geometry and 5 cm^{-1} resolution. The results are presented here in the temperature reduced form [12]. Because of the hygroscopicity the samples with x>0.33 were studied by placing them in a vacuum cell.

RESULTS

Due to the space limitation only a summary of the results is presented here. The dc conductivity, which has been determined from the complex impedance analysis of the frequency dependent ac conductance and capacitance, follows the classical Arrhenius temperature dependence given by [11]:

$$\sigma_{dc} = (A/T) \exp(-E_\sigma/kT),$$

where A and E_σ are the experimentally determined pre-exponential factor and activation energy respectively; k is the Boltzmann constant and T is the absolute temperature. The composition dependence of σ_{dc} is predominantly governed by that of E_σ, as shown in Fig. 1. This figure also

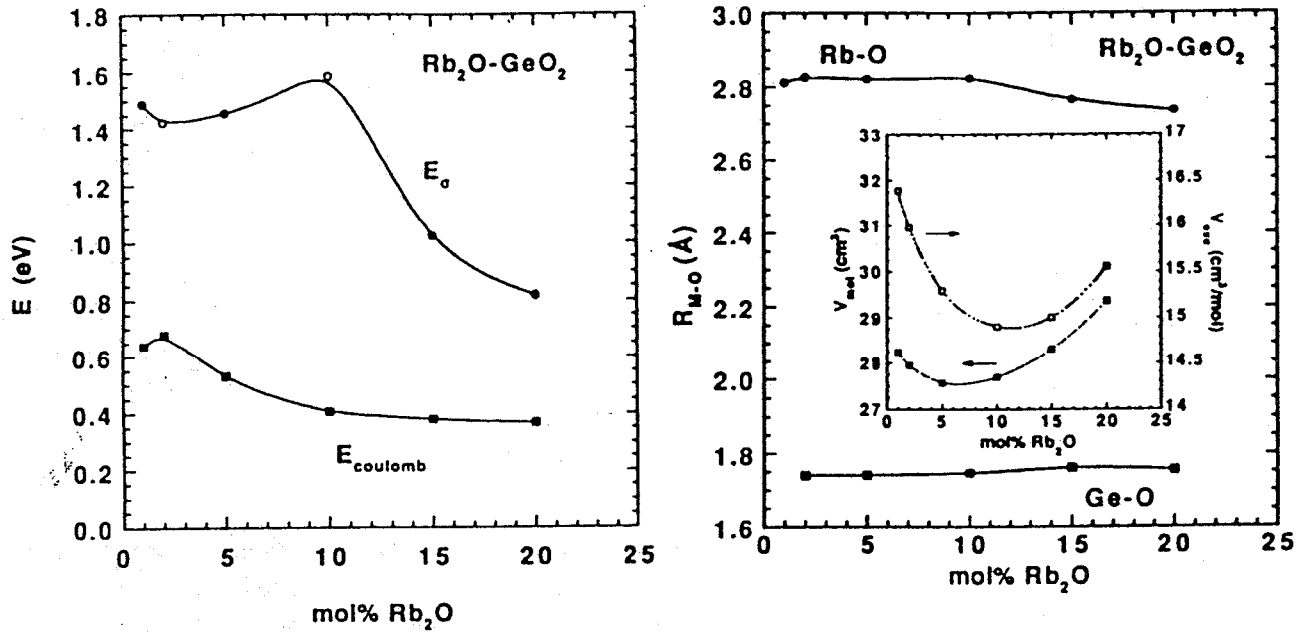

Fig.1. Composition dependence of measured activation energy for dc conductivity, E_σ, and calculated Coulomb energy for ion diffusion, E_{coul}, for $xRb_2O - (1-x)GeO_2$ glass series.
Fig. 2. Composition dependence of interatomic bond distances from Rb (R_{Rb-O} and R_{Ge-O}), and of the molar and excess volumes (V_m and V_{ex}) in the inset.

shows the composition dependence of the Coulomb energy (E_{coul}) between a Rb^+ ion and its neighboring oxygen [11].

The EXAFS results obtained from the analysis of the K-absorption edge of Rb and Ge yield the Rb-O and Ge-O bond distances for this glass series, as shown in Fig. 2 [5]. This figure also shows the composition dependence of the molar volume (V_m), and unoccupied (or excess) volume (V_{ex}); the latter being defined as the space not occupied by the atoms which are treated as hard spheres. The EXAFS analysis also yields the disorder parameter i.e. the mean square displacement for both the bonds. Its value is about an order of magnitude larger for the disorder around Rb than that around Ge. Further, the disorder around Rb decreases by about a factor of two when Rb_2O concentration is increased from 1 to 20 mol%. For the same composition change, the disorder around Ge shows a small increase [5].

From the analysis of O 1s XPS spectrum the relative concentration of non-bridging oxygen (NBO) is determined directly. Assuming that the addition of a Rb_2O unit to GeO_2 either introduces two NBOs for charge compensation or converts a GeO_4 tetrahedron to a GeO_6 octahedron, the fraction of octahedrally coordinated Ge, N_6, is determined (see Fig. 3). The solid line represents the condition that no NBOs are produced with the addition of Rb_2O. These results are consistent with that obtained, albeit with less accuracy, from the increase in Ge-O bond distance associated with the $GeO_4 \rightarrow GeO_6$ conversion (Fig. 2) [5]. The discrepancy of the data in Fig. 3 with the hypothetical line arises from the presence of NBOs. With increasing Rb concentration, the Rb 3d binding energy increases with respect to Ge 3d but decreases with respect to bridging O 1s as a reference [4]. Thus on the average a Rb atom becomes less ionized with respect to its BO neighbor but more ionized with respect to the Ge atoms in the network.

The far infrared spectra show that at low alkali content ($x \leq 0.075$) Rb ions occupy one type of sites (called M sites for medium frequencies), while for higher alkali contents two types of sites (called L and H sites corresponding to relatively low and high frequency bands) exist [13]. The H band constitutes the envelope of the ion motion modes in the crystal. The L band represents additional absorption in the glass as compared to crystals and can be attributed to the motion of ions in "secondary" sites, where coordination number and anionic charge density have not reached yet their optimum crystal-like values as characterized by the H sites. An L band has no crystalline analog. The frequencies of all Rb motion bands ($\nu_L < \nu_M < \nu_H$) increase with Rb_2O content, which is attributed to the increase of anionic charge density of the Rb-hosting sites and to the progressive decrease of the Rb-O distance [13].

The information about the intermediate range structure of the present glasses has been obtained from their Raman spectra which are shown for all the samples in Fig. 4. The major spectral changes with increasing Rb_2O content are noted below together with their interpretation as inferred from the comparison of the present spectra with those of the rutile and quartz forms of GeO_2 and crystalline alkali germanates, and published spectra of silicate glasses. A detailed analysis of the spectral assignments will be given elsewhere [14].

With increasing Rb_2O concentration up to about 30 mol%: (a) The band at ~ 418 cm^{-1} decreases in intensity and almost vanishes at $x=0.25$. It represents the stretching of Ge(4)-O-Ge(4) linkages. Thus the concentration of the tetrahedrally coordinated Ge (i.e. Q^4 structural units, where Q^n indicates a GeO_4 species with n bridging and 4-n non-bridging oxygen atoms) decreases. (b) New bands at ~ 590, 630 and 315 cm^{-1} appear and become stronger, reaching a maximum intensity at $\approx$ 20 mol% Rb_2O. These bands are the characteristics of a structure in which GeO_6 octahedra and GeO_4 tetrahedra link to form a three dimensional network, in analogy to the structure of $Na_4Ge_9O_{20}$ crystal. This structure consists of the Ge(4)-O-Ge(6) and Ge(6)-O-Ge(6) units. (c) A complex band at ~520-530 cm^{-1} which continues to become stronger with increasing Rb_2O content. It is assigned to the symmetric stretching of Ge(4)-O-Ge(4) and Ge(4)-

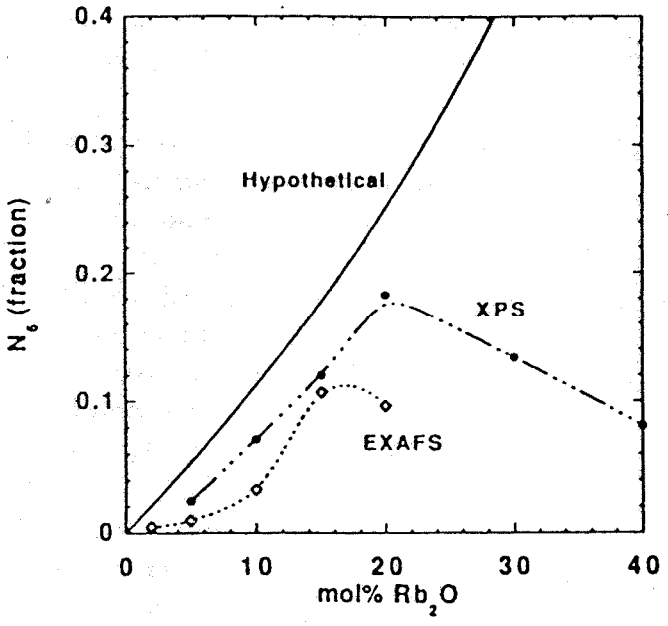

Fig. 3. Composition dependence of the fraction of six-fold coordinated Ge, N_6, for the xRb_2O - (1-x) GeO_2 glass series. The solid line represents hypothetical condition when no NBOs are introduced in the structure. The data are obtained from O-1s XPS spectra.

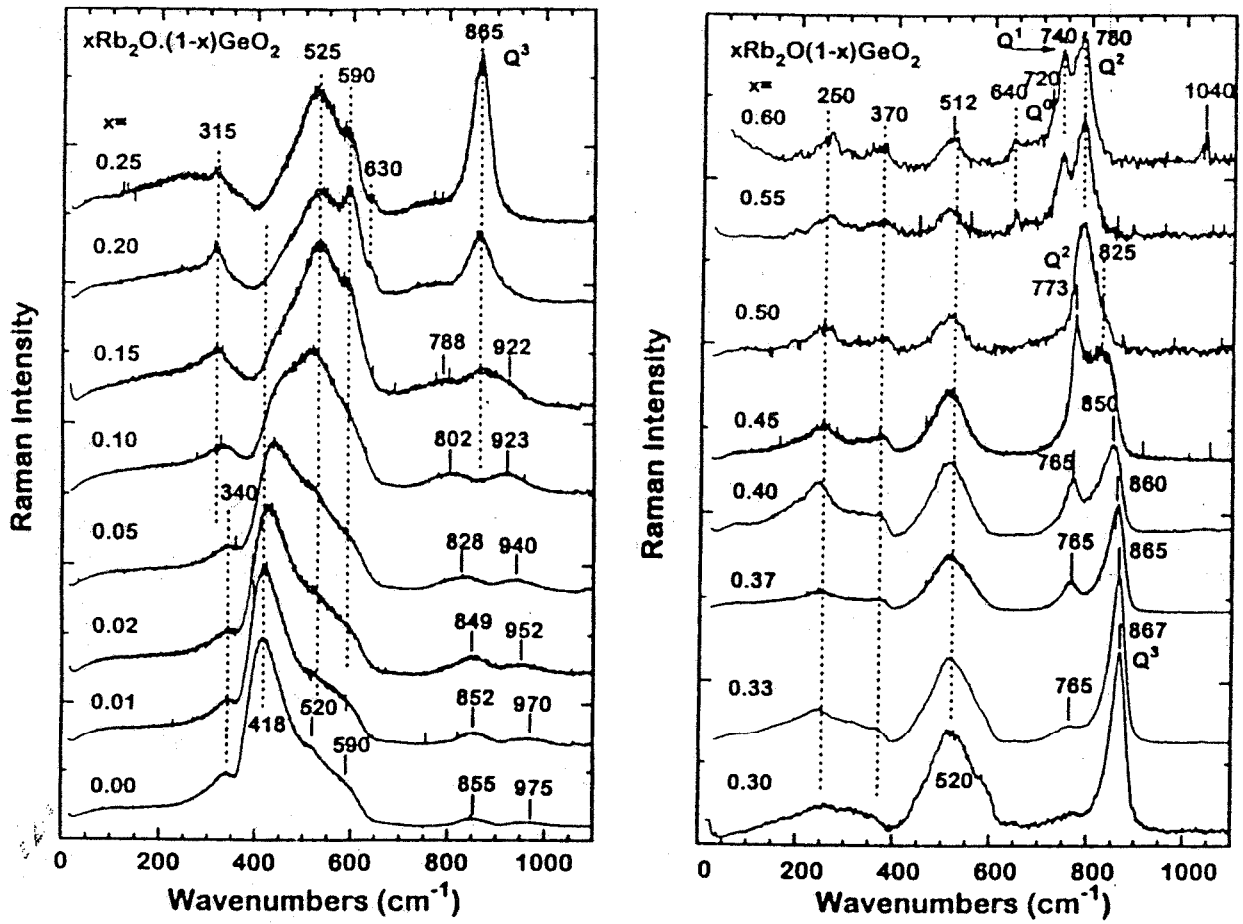

Fig. 4. Raman spectra for the xRb_2O - (1-x)GeO_2 glass series.

O-Ge(6), since a similar band is observed in the spectra of $Rb_2Ge_4O_9$ crystal which consists of a GeO_6 octahedron sharing corners with three membered rings of GeO_4 tetrahedra. This crystal structure includes Ge(4)-O-Ge(4) as well as Ge(4)-O-Ge(6) bridges. (d) The frequency of the doublet at ~855 and 975 cm^{-1} decreases. These bands represent asymmetric stretching of Ge(4)-O-Ge(4) bridges, and a decrease of their frequency indicates that some of the Ge atoms are

converting to six-fold coordination. (e) A new band due to the symmetric stretching of Ge-O$^-$ (where O$^-$ represents an NBO) in Q^3 type GeO_4 tetrahedra appears at ~870 cm^{-1} for x≥0.10.

For Rb_2O concentration >30 mol%, the spectra change predominantly in a different frequency region than that for the lower Rb_2O containing glasses. These changes include: (a) The appearance of new bands due to the symmetric stretching vibrations of the Ge-O$^-$ bonds at 765 cm^{-1} from Q^2 species (for x>0.30), at 740 cm^{-1} from Q^1 species (for x>0.5) and at 720 cm^{-1} from Q^0 species (for x=0.6). (b) The band at ~500 cm^{-1} due to the symmetric stretching of Ge(4)-O-Ge(4) decreases in intensity and frequency. The frequency decrease is ascribed to an increasing inter-tetrahedral angle from increasing number of NBOs per four-coordinated Ge atom. The intensity decrease is due to the decrease in Ge(4)-O-Ge(4) bridges from increasing depolymerization resulting from the formation of NBOs. (c) Two new bands appear at ~250 and 370 cm^{-1} due to the bending modes of Q^2 and Q^1 tetrahedra.

The salient information from the observed changes in Raman spectra is contained in Fig. 5 which shows the compositional dependence of the bands at: (a) 418-445 cm^{-1} representing Ge(4)-O-Ge(4) bridges, (b) 517-530 cm^{-1} representing 3-membered GeO_4 rings, Ge(4)-O-Ge(6) and Ge(4)-O-Ge(4 as in Q^3) species, (c) 590 cm^{-1} and 630 cm^{-1} representing Ge(6)-O-Ge(6) linkages. In addition, for x>0.3 the structure becomes increasingly depolymerized with the successive formation of Q^3, Q^2 and Q^1 species.

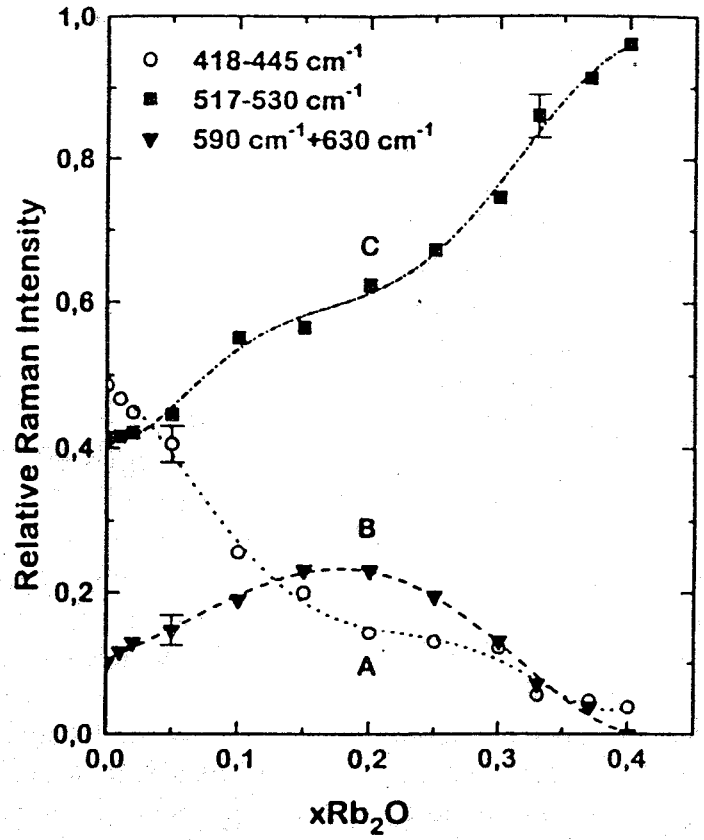

Fig. 5. Composition dependence of selected Raman band intensity for the xRb_2O-(1-x)GeO_2 glass series. Band A at 418-445 cm^{-1}. Band B at 590 and 630 cm^{-1}. Band C at 517-530 cm^{-1}. The lines through the data points are drawn to guide the eye.

DISCUSSION

In general, E_σ for a glass consists of a binding energy term representing the bonding between a cation and its charge compensating center, and a strain energy term representing the dilation of the network needed for an ion to complete its jump [11,15,16]. A calculation of the binding energy approximated by the Coulomb energy does not correlate with the composition

dependence of E_σ [11] (see Fig. 1). Incidentally, the observed variation of the ionicity of Rb ion with composition is indirectly included in E_{coul} via dielectric constant of the medium. So the strain energy appears to be the dominant component of the total activation energy barrier for alkali ion migration in these germanate glasses. In fact, the role of structure on ion transport is most clearly seen in the inverse correlation between E_σ and the molar volume or excess volume. That is, the complex composition dependence of Rb ion transport in Fig. 1 exhibits a correlation with the macroscopic structure in the form of V_{ex} or V_m, rather than with a local structure parameter such as inter-atomic bond distance, local ionicity of the Rb ion, or disorder around Rb (Fig. 2). Earlier Mundy and Gin [17] have explained the change of E_σ with alkali concentration in germanate glasses to arise from the compaction of local network structure from the $GeO_4 \rightarrow GeO_6$ conversion. However, there is a lack of complete correlation between the peak in N_6 in Fig. 3, and E_σ in Fig. 1 or the minimum in V_m or V_{ex} in Fig. 2. Therefore, the composition dependence of local structure is much more complex than previously envisaged. For example, the discrepancy between the solid and experimental curves in Fig. 3 indicates that together with the $GeO_4 \rightarrow GeO_6$ conversion NBOs are simultaneously produced in more or less concentration.

Further insight in the correlation between macroscopic volume and E_σ can be obtained by focusing on the transformation of the structure as given by Figs. 4 and 5. We examine the composition range up to 30 mol% Rb_2O for which E_σ shows maximum variation and complexity. From the nearly monotonic decrease of the intensity of the band 'A' at 418-445 cm^{-1}, it is certain that the linkages of GeO_4 tetrahedra decrease with increasing x at a gradually decreasing rate. In agreement with Fig. 3, the linkages between two GeO_6 octahedra (i.e. the intensity of the bands 'B' at 590 and 630 cm^{-1}) reach a maximum at ~ 20 mol% Rb_2O. These two facts alone do not correlate with, and hence can not explain, the variation of E_σ in Fig. 1.

The sharp decrease of E_σ and the increase of V_{ex} beyond x=0.1 should be most likely due to the expansion of the glass space with the introduction of NBOs, in analogy to the similar observations for the alkali silicates over the *complete* composition range. The situation for the alkali germanates is complicated by the $GeO_4 \rightarrow GeO_6$ conversion dominating up to x=0.2. In this context, note that the intensity of the 'C' band increases slowly with the addition of up to 5 mol% Rb_2O, shows a sharp increase between x=0.05 and 0.1, remains nearly constant up to x=0.15 and then increases rapidly. This is a complex band arising from three kinds of structural units viz. 3-membered rings of GeO_4 tetrahedra, Ge(4)-O-Ge(6) bridge and Ge(4)-O-Ge(4,Q^3) bridge. It is reasonable to assume that the compactness of the structure decreases in the above order for these three units. Also note that the NBOs are produced in significant concentration only for x>0.1 (see the band at 865 cm^{-1} in Fig. 4(a)). These considerations lead us to the following explanation for the behavior of band C, E_σ and V_{ex}: (i) For x<0.1, the addition of Rb_2O breaks up the 3-membered ring structure together with a $GeO_4 \rightarrow GeO_6$ conversion. The intensity of this band increases slowly first because GeO_6 are formed at the expense of the ring structure. We suggest that although the conversion of random GeO_4 units to GeO_6 octahedron may compact the overall structure as indicated by V_{ex} or V_m, the break up of the ring structure opens up the structure slightly in the region through which the Rb ions should pass. (Such an observation could not be made from XPS which does not resolve intermediate range structure.) The small minimum in E_σ between x=0 and x=0.1 is a result of these two competing factors on the scale of intermediate range structure. (ii) Between x=0.1 and 0.15 the intensity of the band does not change much because at this stage the $GeO_4 \rightarrow GeO_6$ conversion continues but at the same time some NBOs are formed at the expense of GeO_6 octahedra. This observation is consistent with the variation of V_{ex} in Fig. 2. It explains why E_σ in Fig. 1 is maximum at x=0.1, but the very sharp decrease of E_σ

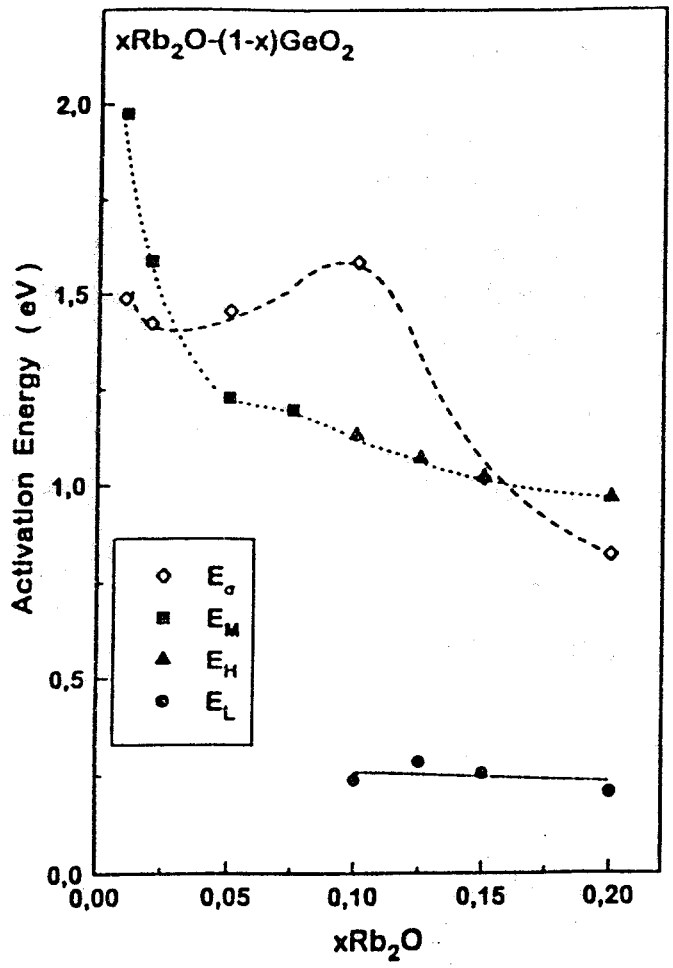

Fig. 6. Comparison of experimentally observed activation energy (E_σ) with that estimated from far IR frequencies (E_M, E_H and E_L) for the xRb_2O-(1-x)GeO_2 glass series.

beyond x=0.1 needs further explanation. It appears that the intermediate range structure is very important for the migration of the ions. It is likely that in this composition range the 3-membered rings, which act as a barrier for the percolation of ions through the structure, disappear completely (iii) The disappearance of GeO_6 and introduction of NBOs become particularly strong at x=0.2 and beyond, as indicated by Fig. 3 and the variation of the intensity of band B in Fig. 4. As expected, V_{ex} increases and E_σ continues to decrease in this region [17]

So far we have not considered the far IR absorption of the samples which represents the local vibrations of Rb cations about their equilibrium site as set by the surrounding structure. Rice and Roth [18] proposed a simple 'free-ion' model according to which E_σ for an ionic crystal is directly related to the far IR absorption frequency ν_{FIR}. Exarhos et al. [19] applied this model to a number of oxide glasses using the following relation:

$$E_\sigma = (M_c d^2 \nu_{FIR}^2)/2$$

where M_c is the mass of the mobile cation and d is the jump distance which may be approximated to nominal Rb-Rb distance. Since we obtain one (ν_M) or two (ν_L and ν_H) far IR absorption peaks depending on whether $x \leq 0.075$ or >0.075, different estimates of the activation energy are obtained depending on the value of ν_{FIR}, as shown in Fig. 6 (E_M, E_L and E_H, respectively) [13]. It is clear that although the activation energy calculated using ν_H or ν_M are comparable with the observed values, there is a qualitative disagreement between the predicted and observed values. This discrepancy has been ascribed to the fact that the strain part of the activation energy from the displacement of the network atoms is not incorporated in the free-ion model [13].

CONCLUSION

The activation energy for dc conductivity (E_σ) of the rubidium germanate glasses is predominantly determined by the strain energy associated with ion hopping rather than the binding energy to break the ion's bond with its charge compensating center. The local structure immediately around the Rb ions (bond distance, degree of disorder) appears to be relatively unimportant for its migration. On the other hand, E_σ shows qualitative correlation with the excess macroscopic volume available in the network structure. The knowledge of the intermediate range structure is shown to be necessary for developing a complete understanding of E_σ. An analysis of Raman spectra suggests that specifically 3-membered GeO_4 rings enhance E_σ. Finally, the 'free-ion' model of ionic conductivity makes a poor prediction of the activation energy of conductivity, because for the present glasses strain energy constitutes a major part of the energy barrier.

Different parts of this work were separately supported by DoE, NATO, NHRF and NSF.

REFERENCES

1. M. D. Ingram, Phys. Chem. Glasses **28**, 215 (1987).
2. H. Jain and C.H. Hsieh, in Diffusion in Amorphous Materials, edited by H. Jain and D. Gupta (TMS, Warrendale, PA, 1994) p. 63.
3. C. H. Hsieh and H. Jain, "Dielectric Constant of Sodium Silicate Glasses in Relation to Their Chemical Structure", these proceedings.
4. X. Lu, H. Jain and W.C. Huang, "Structure of Potassium and Rubidium Germanate Glasses by X-ray Photoelectron Spectroscopy", Phys. Chem. Glasses, in press.
5. W.C. Huang, H. Jain and M.A. Marcus, J. Non-cryst. Solids **180**, 40 (1994).
6. H. Jain, E.I. Kamitsos, Y. Yiannopoulos, G.D. Chryssikos, W.C. Huang, R. Küchler, and O. Kanert, "A Comprehensive View of the Local Structure Around Rb in Rubidium Germanate Glasses", J. Non-cryst. Solids, in press.
7. M.K. Murthy and J. Ip, Nature **201**, 285 (1964).
8. K. Nassau, D.L. Chadwick and A.E. Miller, J. Non-Cryst. Solids **93**, 115 (1987).
9. D.L. Wood, K. Nassau and D.L. Chadwick, Appl. Optics **21**, 4276 (1982).
10. P.P. Lottici, I. Manzini, G. Antonioli, G. Gnappi and A. Montenero, J. Non-Cryst. Solids **159**, 173 (1993).
11. W.C. Huang and H. Jain, J. Non-cryst Solids **188**, 254 (1995)
12. G.E. Walrafen, M.S. Hokmabadi, P.N. Krishnan, S. Guha, R.G. Munro, J. Chem. Phys. **79**, 3609 (1983).
13. E. I. Kamitsos, Y. Yiannopoulos, H. Jain and W. C. Huang, "Correlation Between Far Infrared Absorption and Electrical Conductivity of Rubidium Germanate Glasses", J. Non-cryst. Solids, in press.
14. E. I. Kamitsos, Y. D. Yiannopoulos, M. A. Karakassides, G. D. Chryssikos and H. Jain, "Raman and Infrared Structural Investigation of xRb_2O:(1-x) GeO_2 Glasses", to be published.
15. O.L. Anderson and D.A. Stuart, J. Am. Ceram. Soc. **37**, 573 (1954).
16. C.H. Hsieh and H. Jain, J. Non-cryst. Solids **183**, 1 (1995).
17. J.N. Mundy and G.L. Jin, Solid St. Ionics **24**, 263 (1987) and **21**, 305 (1986).
18. M. J. Rice and W. L. Roth, J. Solid State Chem. **4**, 294 (1972).
19. G. J. Exarhos, P. J. Miller and W. M. Risen, Solid State Commun. **17**, 29 (1975).